Elaboration of a novel glass-to-metal seal for tubular solar receiver

YINGLIANG TIAN, HUI LI*, WENCAI LIU, YANLI SHAO
College of Materials Science and Engineering, Beijing University of Technology, Beijing, 100124, P.R. China

This work aimed at developing a glass-to-metal seal for the tubular receiver in parabolic trough solar power plant. A novel self-developed glass (GD480S) was developed and the sealing structure was optimized by the examination of air tightness, tensile strength, and thermal shock resistance. The results showed that the self-developed glass presented a compliant coefficient of thermal expansion to 4J29 Kovar alloy. An optimized performance was realized using bilateral structure with a sealing length of 3-5 mm. The assembly of the seal using self-developed glass and designed structure can meet the requirement of industrial tubular solar receiver.

(Received November 3, 2014; accepted March 19, 2015)

Keywords: Trough solar power plant, Tubular receiver, Seal, Borosilicate glass

1. Introduction

Parabolic trough solar plant is currently one of the main form of solar energy power generations, which was also a promising alternative to take the place of fossil fuel power plant in industrial heating system, desalination, air-conditioning, refrigeration, chemistry production and irrigation [1,2]. It consisted of massive stacked heat collection elements, each of which utilizes parabolic mirrors to concentrate the sunlight on a tubular receiver where the absorbed solar energy was directly converted into high-pressure steams for heat exchanging [3-5]. As the key component of each element, the tubular solar receiver usually consisted of three parts, an internal steel tube coated with a high selective layer to absorb the solar energy, an outer transparent glass tube, and a ringlike seal that connects the glass tube to the steel. The quality of the glass-to-metal sealing determines the vacuum of the assembly and therefore it plays a decisive role in the energy conversion efficiency and the service life of the heat collection system [6].

In most cases, the hermetic seal is made by a Kovar alloy ring joining to a glass tube. The application of Kovar alloy is primarily due to the compatible coefficient of thermal expansion (CTE, 4.8-5.0×10^{-6} K^{-1}) with glass. Regarding the glass tube, the borosilicate glass 3.3 (CTE, 3.1-3.3×10^{-6} K^{-1}) has been widely used owing to its excellent chemical stability and good thermal shock resistance [7]. However, the wettability of borosilicate glass 3.3 to metal is not satisfied, so that the application of a multi-segment transition tube is always of necessity in order to ameliorate the quality of sealing and to accommodate the mismatch between glass to metal. The drawback of this technical route is that the sealing process becomes more intricate so that the reliability of the sealing joint is greatly decreased. Recently, a comprehensive survey [8] on the operation and maintenance of through solar power plant indicated that the breakage of glass tube resulted from the mismatched glass-to-metal stress in-service is still the main cause of the degradation of system. Therefore, the development of more adapted glass [9] and the improvement of robust seal structure [10, 11] are of great importance in the production of tubular receiver of through solar power plant. In this work, a novel glass material that compromise the thermal expansion property, the chemical stability and wettability to Kovar alloy was developed. The effect of the structure of seal on the bonding quality was examined by the evaluation of tensile strength, air tightness and thermal shock resistance.

2. Experimental

2.1 Materials

The glass-to-metal seal was implemented as same as that one in the production of commercial tubular receiver. The glass tube had a diameter of 125 ± 1 mm with a thickness of 2.4-3.0 mm. The metal ring was made by Kovar alloy 4J29 (Fe-29Ni-17Co) with a diameter of 116mm at length of 32mm. The thickness of the metal ring was optimized at 0.96 mm. Such a thickness, on the one hand, allowed the seal to mechanically sustain the weight of the entire assembly with tolerated distortion, and on the other hand to reduce the mismatched stress to the smallest

possible level.

2.2 Sealing process and sealing joint structure

The sealing process was performed by manually operated flame fusion. Prior to the sealing, both the glass tube and the metal ring were carefully cleaned and prepared. The glass tube was washed using deionized water and then dried by cleaned air. The Kovar alloy ring was firstly cleaned by several successive steps of acid pickling in order to fully remove the surface oxide and oil. Afterwards, it was degassed annealing in hydrogen atmosphere at 1000 ℃ for about 4 hours.

The flame fused sealing process was manually operated on a glass lathe. At the beginning, the rotated Kovar ring was preheated by a flame to about 700-1000℃ until the color of surface became to a little rosy. The glass tube was also rotated and heated. When the color of the glass changed to be red, the rotating Kovar alloy ring was inserted into the softened glass tube. The sealed area was pressed and shaped by using a graphite hammer. After sealing was finished, the assembly of the seal was quickly placed in a furnace heated to 500-560 ℃ for 10-30 min to fully relieve the stress.

Two types of seal structure were considered, i.e., unilateral seal and bilateral seal, as shown in Fig. 1. In the unilateral-type sealing, the glass tube was cladded on the outer surface of the metal ring. While in the bilateral structure, the blade of the metal ring was fully enwrapped by glass. Although the fuse-sealing process was operated by a skilled operator, the sealing length cannot be precisely controlled within one millimeter. Therefore, four different lengths of sealing were applied, namely, 1-3 mm, 3-5 mm, 5-7 mm, 7-9 mm, respectively. For each condition, a total of 300 seals were prepared with the purpose of minimizing the dispersion of the test results. Among them, each 100 samples were subjected to vacuum-tight test, tensile strength test and thermal shock test, respectively.

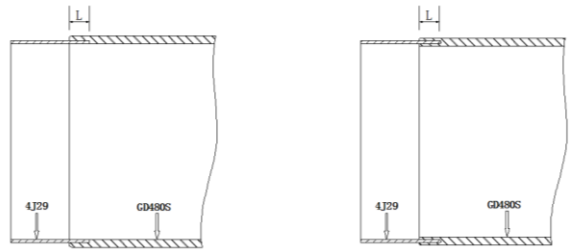

(a) Unilateral sealing (b) bilateral sealing

Fig. 1. Schematic illustration of the sealing joint.

2.3 Characterization

In order to characterize the microstructure of the seal, the sample was firstly cut into small pieces and then immersed into resin to be cured. Later the prepared sample was grinded and polished to a mirror finish. The optical microscope (Olympus I3) and a desktop-type scanning electronic microscope (Phenom ProX) were applied to observe the cross-sectional microstructure of the seal.

The vacuum-tight of the seal was detected by using helium mass spectrometer leak detector (ZHP-30, KYKY Technology Ltd., China). Helium has the characteristics of small viscosity, non-toxic, chemically inert and therefore was used as a tracer penetrating small leaks rapidly.

The bonding strength of the seal was characterized by a pull-out test using a universal testing machine (model, CMT4304, MTS China). The maximum force of the machine is 30kN. Prior to the tensile test, both the two surface of seal was glue to a self-made fixture and then cured at 60-80℃ for 30 minutes. The fixture allowed a good alignment of the glass tube and the Kovar alloy ring during tensile testing, as shown in Fig. 2. During the test, the assembly of the sample was pulled out at a constant displacement velocity of 5 mm/min until failure occurred. Finally, the tensile strength of the sample was obtained according to the equation (1)

$$\sigma = \frac{F}{\pi R^2 - \pi r^2} \tag{1}$$

where F is the loaded force, R and r are the outside radius and the inside radius of glass tube, respectively.

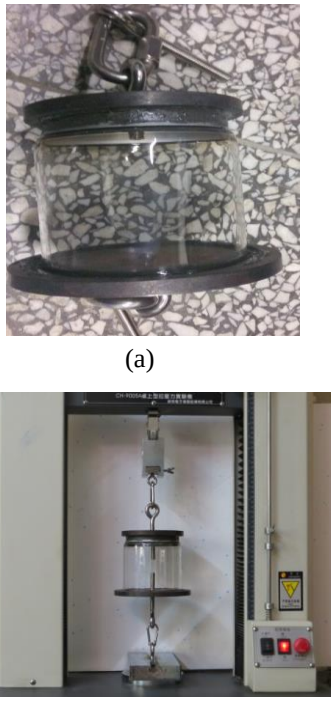

(a)

(b)

Fig. 2. The tensile test fixture (a) and the installed assembly (b).

The thermal shock resistance was tested in accordance with the standard thermal cycling procedure for laboratory glassware (GB/T 6579-2007, ISO718:1990 [12]). In each cycle, the sealed assembly was firstly heated to 230℃ in a vertical furnace with holding time of 30 minutes. Then the bottom of the furnace was opened allowing a number of samples dropped directly into the water basin. The quenched sample was then collected and dried for both the visual observation using magnified glass and the leakage detection. If any crack occurred or leakage happened, the sample was determined to be failure and the number of thermal cycling was recorded for the evaluation of thermal shock resistance.

3. Results and discussion

3.1 Characteristics of the self-developed GD480S glass

The design concept of GD480S glass was based on the typical borosilicate glass, whose main ingredient includes SiO_2, Al_2O_3, B_2O_3, and a small amount of alkali metal oxide (R_2O). Among them, both SiO_2 and B_2O_3 provide the necessary glassy network unit. The role of B_2O_3 lies in the reduction of melting temperature, the enhancement of chemical stability and the decrease of thermal expansion coefficient. The content of R_2O in the glass was carefully optimized to regulate the coefficient of thermal expansion of glass. Table 1 lists the proprietary composition [13] of the self-developed glass. For confidential reason, only the range of the formulation is given here. The composition of borosilicate glass 3.3 is also listed in the table for the sake of reference. The heating induced linear extension rate of both the self-developed glass (GD480S) and Kovar alloy (4J29) is displayed in Fig. 3. The averaged thermal expansion coefficient of the self-developed GD480S glass is 4.83×10^{-6} K^{-1}. The glass soften point is in the range of 480-520 ℃ depending on the ingredient constitution which is slight higher than the curie point of 4J29. Moreover, two distinct thermal expansion behaviors was differentiated below and above the temperature of 430℃ for the Kovar alloy 4J29, namely the curie point. Below the curie point of 4J29, the glass GD480S presented a very similar characteristic of thermal expansion with respect to the Kovar alloy. It can be reasonable speculated that the thermal induced mismatch stress either originated from the fuse-sealing process or generated in the thermal cycling in-service can be markedly reduced.

Table 1. The chemical composition of the self-developed glass (GD480S) and glass 3.3 (wt.%).

	SiO_2	Al_2O_3	B_2O_3	R_2O	Fe_2O_3	other
glass 3.3	80.2	2.3	12.7	4.07	< 0.05	0.2
GD480S	68-72	2-4	15-18	7-9		

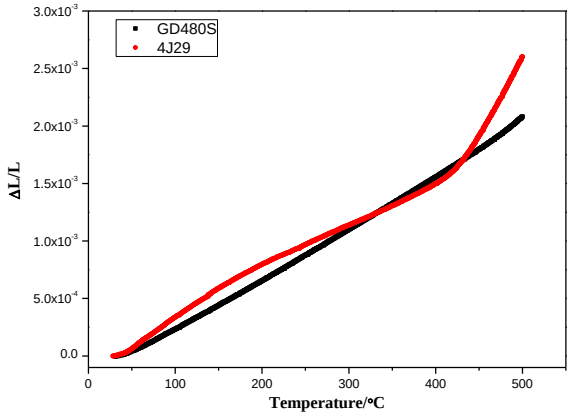

Fig. 3. Linear extension rate with the function of temperature of Kovar alloy 4J29 and the self-developed glass (GD480S).

3.2 Microstructure of the sealing joint

Fig. 4 displays the sectional view of the seal with two different joint structures. The interface between the glass and the metal ring is very compact and dense, indicating a good wetting condition between them. The further observation on the interface of the seal was performed on a desktop-type SEM equipped with EDS, as shown in Fig. 5. A mixed zone in the metal-glass interface measuring approximately 10 μm can be clearly identified. The line scan of EDS (Fig. 5b, c) suggested that the oxidation of Kovar (Fe-Ni-Co) alloy on the alloy surface and merged with the fully fused outer glass. In addition, some sporadically fused iron alloy oxide allowed the melting glass deeply penetrating into the grain boundary. These observations give an indication of good metallurgical bonding formed at the interface of the seal.

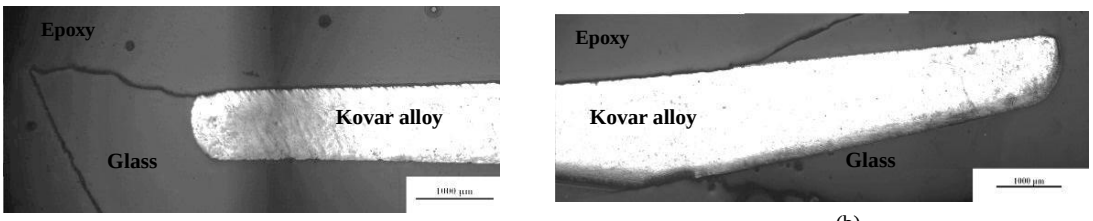

(a) (b)

Fig. 4. Cross section of the glass-to-metal sealing joint (a) unilateral sealing, (b) bilateral sealing.

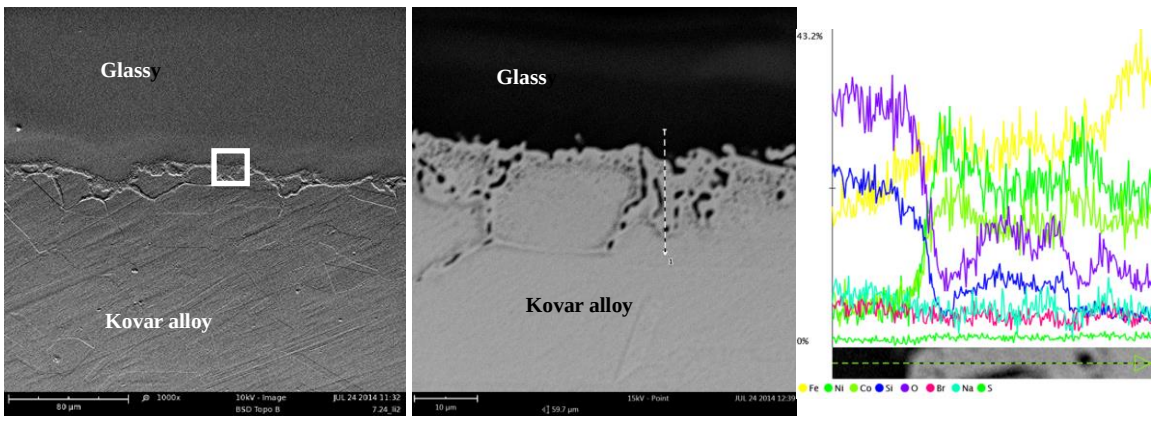

(a) (b) (c)

Fig. 5. Interface observation of the bilateral sealing joint (a), (b) is the magnified observation on the box zone of (a) and (c) is the element distribution of the scanned line indicated in (b).

3.3 Non-leakage reliability of the seal

For each process condition, the air tightness testing was conducted for a total of 100 samples. The number of the leaked sample was counted and recorded as the percentage of leakage. The relationship of the sealing length with regard to the leakage rate is illustrated in Fig. 6. For the seal where only limited area was bonded at the glass-to-metal interface, i.e., short sealing length (e.g. 1-3 mm) and/or single side of the metal blade was sealed with glass, air leakage is prone to occur. With the increase of the sealing length, the leakage rate dropped significantly and it reached to zero when the sufficient length of sealing was guaranteed (e.g. 7-9mm). The result also confirmed that the bilateral-type seal displayed better performance in air tightness compared to the unilateral structure because of the improvement of bonding quality between glass and metal.

3.4 Tensile strength of the assembly of the sealing joint

The tensile strength of the sample was statistically analyzed by using two-factor weibull distribution [14]. The result was drawn in Fig. 7 where the X-coordinate represents the logarithmic value of the tensile strength (σ) and the Y-coordinate is the Weibull function of the probability density of tensile strength (A). Each line in the figure represents the Weibull distribution of tensile strength of the seal under one process condition, whose slope indicated the Weibull modulus that the greater the slope the more reproducibility of the tensile strength. It can be seen that the distribution of tensile strength was divided into two regions. When the sealing length is too small (1-3 mm) or too long (7-9 mm), it is always the seal that fractured and the tensile strength is relatively low (<10 MPa). The bonding strength of the seal with appropriate sealing length was increased markedly, even larger than the tensile strength of glass tube. As a consequence, failure occurred at the glass whose tensile strength was in the range of 12.3-12.7 MPa. In this case, one can hardly recognize the effect of the processing conditions on the result of tensile strength.

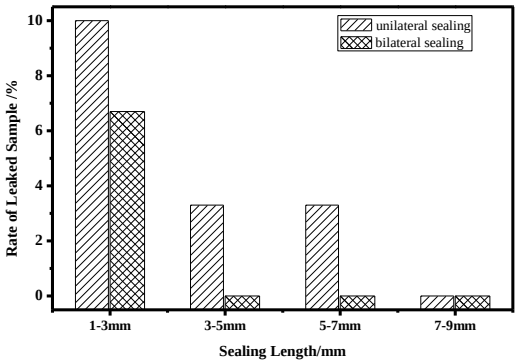

Fig. 6. The dependence of the rate of leakage on the sealing length.

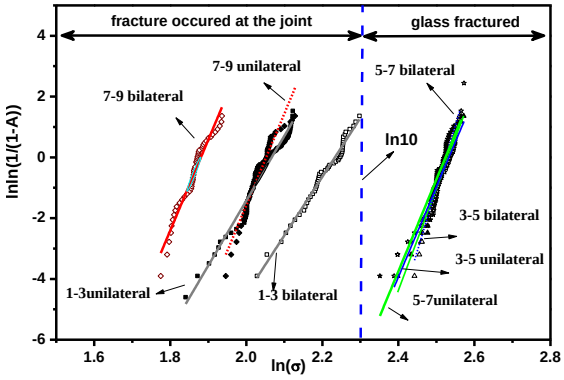

Fig. 7. Weibull distribution of the tensile strength of the joint under different conditions.

For the seal with the shortest sealing length (1-3 mm), the bilateral structure presented better performance (8.9-9.4 MPa) than unilateral-type sealing (7.6-7.9MPa). This can be explained by the enhancement of the bonding area between the glass and metal. However, with the increase of sealing length, the glass suffered more and more constraint exerted by the embedded metal blade. The negative effect induced by the mismatched stress became more and more important that adversely affected the bonding strength of the seal. That is probably the reason why the unilateral-structure seal exhibited higher tensile strength than the counterpart when 7-9 mm length of the metal ring was sealed to the glass.

3.5 Thermal shock resistance of the seal

Fig. 8 shows the dependence of thermal shock resistance on the seal structure and length of the sealing, which was also evaluated by Weibull distribution. Roughly speaking, the higher value of thermal shock resistance was achieved at the shortest seal (1-3 mm) regardless of the joint structure. With the increase of the sealing length, the thermal shock resistance was gradually declined. Moreover, it was found that fracture occurred at the glass side for the majority of damaged sample, approximately 10 mm away from the seal, as shown in Fig. 9a. This was probably related to the local stress concentration. Fig. 9b gives a representative example of the residual stress distribution of the seal, which was qualitatively characterized by using a glassware stress detector (LZY-150, China). The blue color shown in the figure is the presence of internal stresses while the purple area is a low stressed zone. The residual stress accumulated in the thermal cycling was very sensitive to the constraint condition. For the seal with longer sealing length, the constraint that the metal alloy blade exerted on the glass became increasingly important that resulted in greater internal stress during the subsequent thermal cycles.

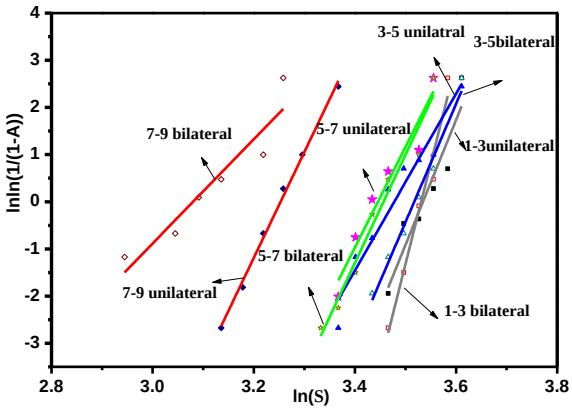

Fig. 8. Weibull distribution of the shock resistance of the joint under different conditions.

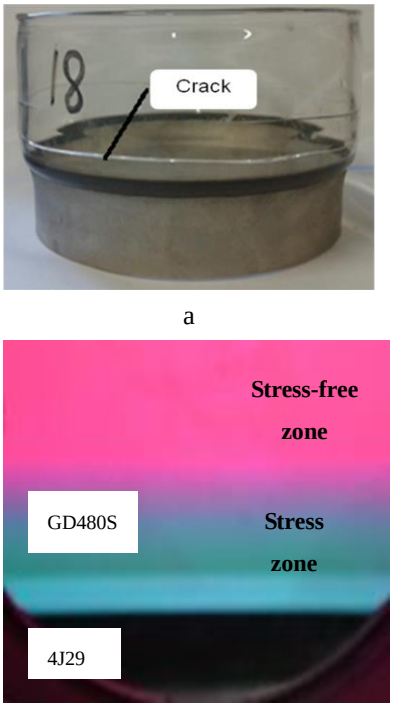

Fig. 9. The failure sample after thermal cycling and the distribution of stress of the sealing joint.

Although the self-developed glass presented a very close coefficient of thermal expansion with respect to Kovar alloy, care should still be taken on the seal structure and the sealing length. Because the metal part that possess much higher thermal conductivity always cools faster than the glass part, the temperature difference between glass and metal during thermal cycles would also contribute to the generation of restraint stress. Therefore, in order to meet the multiple requirements of industrial tubular receiver, as a prerequisite of air tightness and bond strength, it is better using bilateral structure with short length of sealing (i.e. 3-5 mm) to ensure the good thermal shock resistance of the seal.

4. Conclusions

In this work, a novel glass (GD480S) and the seal structure applied for the tubular thermal receiver was developed. The performance and reliability of the seal was examined by air tightness test, tensile test, and thermal shock test. The self-developed GD480S glass possessed a closed thermal expansion coefficient with Kovar alloy. The bilateral structure of seal with a length of 3-5 mm exhibited the optimized overall performance. The tensile testing results showed that the bonding strength of the seal was superior to the strength of glass under the optimized process conditions. The self-developed seal can meet the multiple requirement of industrial application, including the reliability of air tightness and thermal shock resistance.

Acknowledgement

The financial support by the project of Natural Science Foundation of China (No. 51271007) is gratefully acknowledged.

References

[1] A. Fernandez-Garcia, E. Zarza, L. Valenzuela, M. Perez, Renew. Sust. Energ. Rev. **14**, 1695 (2010).
[2] A. Hepbasli, Z. Alsuhaibani, Renew. Sust. Energ. Rev. **15**, 5021(2011).
[3] C. Xu, Z. F. Wang, X. Li, F. H. Sun, Appl. Therm. Eng. **31**, 3904 (2011).
[4] A. Ghobeity, C. J. Noone, C. N. Papanicolas, A. Mitsos, Sol. Energy. **85**, 2295 (2011).
[5] D. Mills, Sol. Energy. **76**, 19 (2004).
[6] D. Q. Lei, Z. F. Wang, J. Li, J. B. Li, Z. J. Wang, Renew. Energy. **48**, 85 (2012).
[7] B. Danick, W. Patrick, F. R. Nicolaas, Sensor. Actuator. **114**, 543 (2004).
[8] H. Price, E. Iüpfert, D. Kearne, J. Sol. Energy Eng. **124**, 109 (2002).
[9] D. Q. Lei, Z. F. Wang, J. Li, Mater. Design. **31**, 1813 (2010).
[10] N. Benz, F. D. Doenitz, T. Kuckelkorn, Proc. 12-th solar PACES, Oaxaca, Mexico, 2004, p. 885.
[11] H. Price, M. J. Hale, R. Mahoney, Proc. ISEC2004: Intern. Solar Energy Conf., Portland, Oregon, USA, 2004, p. 659.
[12] ISO718:1990 Laboratory glassware-Methods for thermal shock tests.
[13] Y. L. Tian, X. H. Liang, X. L. Guo, S. B. Sun, China Patent, 201110235743.3, 2011.
[14] S. Raif, A. Irfan, Mater. Design. **29**, 1170 (2008).

*Corresponding author: hui.li@bjut.edu.cn